JOURNAL OF COMPUTATIONAL PHYSICS 55, 98–114 (1984)

An Effective Vorticity–Vector Potential Formulation for the Numerical Solution of Three-Dimensional Duct Flow Problems

A. K. WONG AND J. A. REIZES

School of Mechanical and Industrial Engineering,
The University of New South Wales,
Kensington, New South Wales, Australia 2033

Received February 22, 1983; revised July 12, 1983

The Vector and Scalar Potential formulation for the numerical solution of laminar incompressible through-flow problems is reviewed. Some deficiencies of this method are discussed, and in particular a subtle but serious problem associated with the Scalar Potential is unveiled. An improved Vorticity–Vector Potential formulation is then presented for incompressible flows in ducts of constant but arbitrary cross sections. The method features a new irrotational component of velocity which essentially removes the problem source by eliminating the necessity of a Scalar Potential.

1. INTRODUCTION

The modelling of viscous flow development in tubes and ducts has been a subject of extensive research for some time. Early attempts include the noted work of Langhaar [1], who developed a linearization technique for the Navier-Stokes equations, and successfully obtained an approximate solution for incompressible laminar flow development in a circular tube. Han [2] later extended this technique to flows in the entrance region of rectangular ducts. Since then, there have been numerous studies devoted to this subject, many of which include analyses in three dimensions, (e.g., Sparrow *et al.* [3], Carlson and Hornbeck [4] and Ghia *et al.* [5]).

Unlike numerical studies in two dimensions, in which the use of the vorticity-stream function is by far the most popular approach (see [6]), 3-D duct flow analyses have almost invariably been tackled by the pressure–velocity formulations. Although the existence of a 3-D analogue of the stream function, referred to as the Vector Potential, has been known for over a century, its first successful implementation was not achieved until 1967 when Aziz and Hellums [7] solved the natural convection problem using this derived variable. The main reason for such a long delay has been due to the confusion involved in the determination of a set of suitable boundary conditions for the Vector Potential. First to resolve this problem were Hirasaki and Hellums [8], who formally derived a set of appropriate boundary conditions for a general hydrodynamic flow field. Their formulation was relatively simple for

0021-9991/84 $3.00

confined-flow problems, which incidentally verified the correctness of the Aziz and Hellums model, but its extension into through-flow situations was much too complex to be useful. In a later paper, however, Hirasaki and Hellums [9] showed that simple boundary conditions are possible if a Scalar Potential is introduced to account for the through-flow velocities. But an obvious setback from this approach is the added burden on both the computational time and storage required in dealing with the additional variable. Another, less obvious but equally serious, problem is related to the effect of the Scalar Potential on the equation of continuity.

It is the purpose of this paper to highlight some of the difficulties associated with the Vector/Scalar Potential formulation, and in particular to demonstrate that the presence of the Scalar Potential can in fact destroy the advantages inherent in the Vector Potential. A new formulation of the Vorticity–Vector Potential approach to the full 3-D Navier–Stokes equations for flows in ducts of arbitrary but constant cross section is then presented and shown to be superior to its predecessor.

2. The Vector and Scalar Potential Formulation

The equations of motion for viscous incompressible laminar flow in non-dimensional vector form are

$$\frac{\partial \mathbf{V}}{\partial t} + (\mathbf{V} \cdot \nabla)\,\mathbf{V} = -\nabla p + \left(\frac{1}{Re}\right) \nabla^2 \mathbf{V} + \mathbf{F} \tag{2.1}$$

and

$$\nabla \cdot \mathbf{V} = 0, \tag{2.2}$$

where $\mathbf{V} = (u, v, w)$ is the velocity vector, p is the pressure, Re is the Reynolds number and $\mathbf{F}$ is the body force.

By taking the curl of Eq. (2.1), the pressure term is eliminated, yielding the vorticity transport equation

$$\frac{\partial \boldsymbol{\zeta}}{\partial t} + (\mathbf{V} \cdot \nabla)\,\boldsymbol{\zeta} - (\boldsymbol{\zeta} \cdot \nabla)\,\mathbf{V} = \left(\frac{1}{Re}\right) \nabla^2 \boldsymbol{\zeta} + \nabla \times \mathbf{F}, \tag{2.3}$$

in which the vorticity $\boldsymbol{\zeta}$ is defined as

$$\boldsymbol{\zeta} = \nabla \times \mathbf{V}. \tag{2.4}$$

For incompressible laminar flow, Hirasaki and Hellums [9] showed that it is possible to express the velocity field in terms of the curl of a Vector Potential $\boldsymbol{\psi}$ and the gradient of a Scalar Potential ϕ, such that

$$\mathbf{V} = \nabla \times \boldsymbol{\psi} + \nabla \phi. \tag{2.5}$$

Noting that $\nabla \cdot (\nabla \times \boldsymbol{\psi}) \equiv 0$, the substitution of Eq. (2.5) into Eq. (2.2) leads to

$$\nabla^2 \phi = 0. \tag{2.6}$$

The relation between $\boldsymbol{\psi}$ and $\boldsymbol{\zeta}$ is established by taking the curl of Eq. (2.5) which yields

$$\nabla(\nabla \cdot \boldsymbol{\psi}) - \nabla^2 \boldsymbol{\psi} = \boldsymbol{\zeta}. \tag{2.7}$$

It may be shown that a solenoidal solution of $\boldsymbol{\psi}$ is always possible, so that following Aziz and Hellums [7], Eq. (2.7) is reduced to

$$\nabla^2 \boldsymbol{\psi} = -\boldsymbol{\zeta}. \tag{2.8}$$

It has already been demonstrated [9] that if the Scalar Potential were used to deal with the through-flow velocities, then simple boundary conditions on $\boldsymbol{\psi}$ are possible. Thus by setting

$$\frac{\partial \phi}{\partial n} = -\hat{\mathbf{n}} \cdot \mathbf{V} \tag{2.9}$$

on the boundaries, where $\hat{\mathbf{n}}$ is the outward drawn unit normal, the boundary conditions on $\boldsymbol{\psi}$ for a simply connected region may be shown to be

$$\psi_t = \frac{\partial \psi_n}{\partial n} = 0, \tag{2.10}$$

where subscripts t and n denote tangential and normal components, respectively.

In principle, the Vector and Scalar Potential $(\boldsymbol{\psi}, \phi)$ formulation provides an effective means of solving 3-D flow problems. In practice, however, this approach does suffer from certain drawbacks, some of which were discussed by Roache [10]. One well-known disadvantage is the increased number of equations to be handled. In working with the primitive variables $(p, \mathbf{V})$, it is usual to solve three momentum equations, a pressure equation and, typically, one other equation to correct for a non-zero dilatation (see, for example, [11, 12]). In the $\boldsymbol{\psi}$, ϕ method, there are three vorticity transport equations, three Poisson equations for the Vector Potential and a Laplace equation for the Scalar Potential. Admittedly in the p, $\mathbf{V}$ system, the pressure equation, being more involved and with mostly non-homogeneous derivative boundary conditions, is difficult to solve. But for 3-D computational studies, memory requirement tends to govern the feasibility of implementing a particular numerical scheme. It is therefore understandable that techniques which deal with the least number of variables have been strongly favoured.

In using the $\boldsymbol{\psi}$, ϕ formulation, Aregbesola and Burley [13] reduced somewhat the computational time required by assuming a known exit velocity profile, so that ϕ needed to be solved only once. However, this technique does not ease the memory requirement, and would not be applicable if the problem were extended to include

heat transfer, or to ducts of arbitrary cross sections where the outlet velocity profile is not known a priori.

Another problem associated with this technique is of a numerical nature. It is well known that the $\nabla \times \boldsymbol{\psi}$ component of velocity satisfies the equation of continuity in the finite difference form irrespective of the accuracy of the solution for $\boldsymbol{\psi}$. The same, however, cannot be said about the $\nabla\phi$ component. Consider the meshing scheme as shown in Fig. 2.1 and assume that the central difference form of the Laplace equation $\nabla^2\phi = 0$ may be solved exactly, so that at any node (i, j, k),

$$\frac{\phi(i+1) - 2\phi + \phi(i-1)}{\Delta x^2} + \frac{\phi(j+1) - 2\phi + \phi(j-1)}{\Delta y^2} + \frac{\phi(k+1) - 2\phi + \phi(k-1)}{\Delta z^2} = 0. \tag{2.11}$$

Note that for clarity, the default values (i, j, k) are omitted, e.g., $\phi(i, j, k+1)$ is written as $\phi(k+1)$.

Let $\mathbf{V}' = (u', v', w')$ be the irrotational part of the velocity field, that is, $\mathbf{V}' = \nabla\phi$. Then the components of $\mathbf{V}'$ expressed in central difference form become

$$u' = \frac{\phi(i+1) - \phi(i-1)}{2\Delta x},$$
$$v' = \frac{\phi(j+1) - \phi(j-1)}{2\Delta y}, \tag{2.12}$$
$$w' = \frac{\phi(k+1) - \phi(k-1)}{2\Delta z}.$$

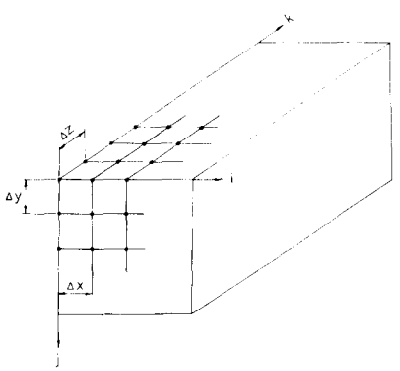

FIG. 2.1. Meshing scheme

Since the divergence of $\mathbf{V}'$ in central difference form is given by

$$\nabla \cdot \mathbf{V}' = \frac{u'(i+1) - u'(i-1)}{2\Delta x} + \frac{v'(j+1) - v'(j-1)}{2\Delta y} + \frac{w'(k+1) - w'(k-1)}{2\Delta z}, \tag{2.13}$$

the substitution of Eqs. (2.12) into Eq. (2.13) leads to

$$\nabla \cdot \mathbf{V}' = \frac{\phi(i+2) - 2\phi + \phi(i-2)}{(2\Delta x)^2} + \frac{\phi(j+2) - 2\phi + \phi(j-2)}{(2\Delta y)^2} + \frac{\phi(k+2) - 2\phi + \phi(k-2)}{(2\Delta z)^2}. \tag{2.14}$$

Simple inspection reveals that the above is not identical to the LHS of Eq. (2.11). It therefore follows that $\nabla \cdot \mathbf{V}'$, and hence $\nabla \cdot \mathbf{V}$, will not in general vanish even if the finite difference form of $\nabla^2\phi$ is exactly zero. This is particularly true in regions where ϕ exhibits high rates of local variation. For flows in a rectangular duct, with boundary conditions used by Aregbesola and Burley, such local variations are indeed found to exist near the exit region of the duct. We note, however, that Eq. (2.14) is simply the finite difference Laplacian of ϕ based on a mesh configuration of $2\Delta x$, $2\Delta y$ and $2\Delta z$. It is therefore of some comfort to know that if the mesh size were made increasingly small, then $\nabla \cdot \mathbf{V}'$ as given by Eq. (2.14) would approach zero. But the significance of the above illustration is that the introduction of the Scalar Potential does in fact destroy the real advantage of using the Vector Potential, which is to assure local and global continuity irrespective of the chosen mesh-size. Further, the selection of a suitable small mesh is restricted, at least for the present, by computer capabilities.

To investigate this problem, the duct flow example in [13] was solved using a

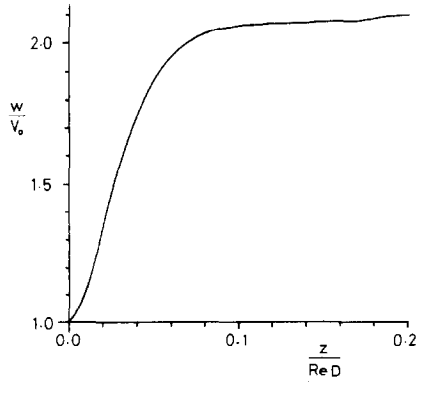

FIG. 2.2. Axial velocity development (ψ, ϕ formulation). Re = 10, $x = 0.5D$, $y = 0.5D$.

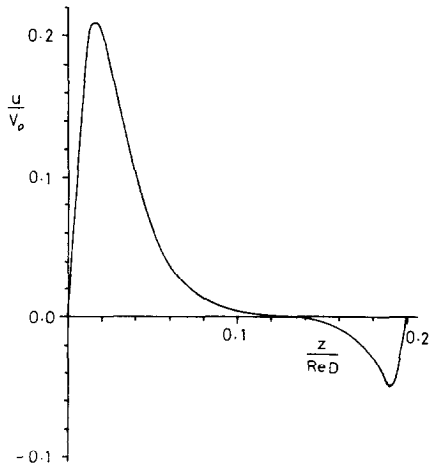

FIG. 2.3. Transverse velocity development (ψ, ϕ formulation). Re = 10, $x = 0.25D$, $y = 0.5D$.

$9 \times 9 \times 17$ mesh scheme at a Reynolds number of 10. The resulting discretized dilatation was indeed quite unacceptable for computational nodes near the exit. This was clearly illustrated by the unreasonable variations in all three velocity components in this region as may be seen in Figs. 2.2 and 2.3. When the mesh was extended to $17 \times 17 \times 33$, the error in the axial velocity was made less obvious, but non-sensical transverse velocities similar to those shown in Fig. 2.3 still appeared near the exit. It is our opinion that in order to achieve any reasonable results with this formulation a scheme with a minimum of 30 mesh points in each direction is required. This limit would of course have to be raised if the Reynolds number were increased.

The necessity for maintaining a fine grid spacing, particularly near the exit, imposes yet another extremely serious, and perhaps cripling, restriction when dealing with duct flows. Unlike the $(p, \mathbf{V})$ formulations where mesh transformation techniques are commonly employed to provide efficient use of grid points, it has been shown in the above example that the ψ, ϕ formulation does not permit the mesh intervals along the axial direction to be progressively spread out.

3. A New Formulation

In view of the difficulties discussed in Section 2, a new formulation was devised for incompressible flows in ducts of constant cross section. The proposed method introduces a new irrotational component of velocity, $\mathbf{w}_0$ in place of $\nabla\phi$, where $\mathbf{w}_0$ $(= \mathbf{w}_0(x, y))$ is simply the normal component of the specified inlet velocity vector. The velocity field $\mathbf{V}$ may now be written as

$$\mathbf{V} = \nabla \times \boldsymbol{\psi} + \mathbf{w}_0. \tag{3.1}$$

An immediate observation from this definition of $\mathbf{V}$ is that the need to solve for ϕ is eliminated. It is also important to note that computational storage is consequently reduced. A saving of $L \times M \times N$ storage locations is achieved where L, M and N are the number of mesh points in the three spatial directions. Further, since

$$\nabla \cdot \mathbf{w}_0 = \frac{w_0(k+1) - w_0(k-1)}{2\Delta z} \equiv 0, \tag{3.2}$$

the divergence of the irrotational component of velocity and its discretization are exactly zero. Hence, the continuity equation in finite difference form is now identically satisfied. By making this simplification, the problems discussed in Section 2 are effectively removed. Although it can easily be seen that neither the vorticity transport equation, Eq. (2.3), nor the relationship between ψ and ζ, Eq. (2.8), is affected, the boundary conditions on ψ remain to be determined.

Boundary Conditions on ψ

Consider the solution region as shown in Fig. 3.1. Here S_i, $i = 1$ to 6, are plane surfaces confining the region.

Let S_1 and S_2 be the inlet and outlet planes of the duct, respectively, and S_3 to S_6 are impermeable solid surfaces representing the duct boundaries. Then the conservation of mass requires that

$$\oiint_{S_i} \mathbf{V} \cdot d\mathbf{S}_i = 0, \qquad i = 3, 4, 5, 6, \tag{3.3}$$

and

$$\sum_{i=1}^{2} \oiint_{S_i} \mathbf{V} \cdot d\mathbf{S}_i = 0. \tag{3.4}$$

Equations (3.3) and (3.4) can be used to determine the boundary conditions.

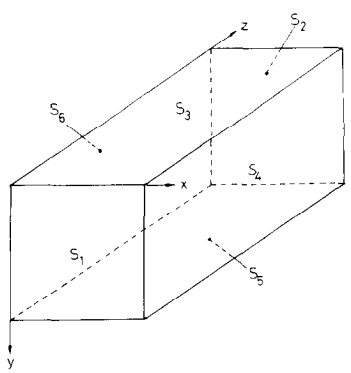

FIG. 3.1. Solution region.

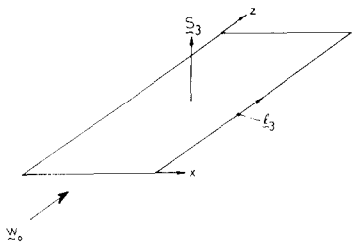

FIG. 3.2. Surface S_3.

(a) *Solid Boundaries*

Consider, for example, the solid surface S_3 as shown in Fig. 3.2. The substitution of Eq. (3.1) into Eq. (3.3) yields

$$\oiint_{S_3} (\nabla \times \boldsymbol{\psi} + \mathbf{w}_0) \cdot d\mathbf{S}_3 = 0. \tag{3.5}$$

Since $\mathbf{w}_0 \cdot d\mathbf{S}_3 = 0$ on S_3, Eqs. (3.5) may be reduced to

$$\oiint_{S_3} (\nabla \times \boldsymbol{\psi}) \cdot d\mathbf{S}_3 = 0. \tag{3.6}$$

By Stokes Theorem, the above equation becomes

$$\oiint_{S_3} (\nabla \times \boldsymbol{\psi}) \cdot d\mathbf{S}_3 = \oint_{l_3} \boldsymbol{\psi} \cdot d\boldsymbol{l}_3 = 0, \tag{3.7}$$

where l_3 is the contour bounding S_3.

This, together with $v = d\psi_x/\partial z - \partial\psi_z/\partial x = 0$ everywhere on S_3, is satisfied if the tangential components of $\boldsymbol{\psi}$ are zero on that surface. Further, since $\boldsymbol{\psi}$ is required to be solenoidal, it can be deduced that an appropriate set of boundary conditions for S_3, and by the same token for S_5, is

$$\psi_x = \psi_z = \frac{\partial \psi_y}{\partial y} = 0. \tag{3.8}$$

Similarly, the boundary conditions for S_4 and S_6 may be shown to be

$$\psi_y = \psi_z = \frac{\partial \psi_x}{\partial x} = 0. \tag{3.9}$$

(b) *Inlet Boundary*

For the inlet plane, the substitution of $\mathbf{V} = \mathbf{w}_0$ into Eq. (3.1) leads directly to

$$\nabla \times \boldsymbol{\psi} = 0. \tag{3.10}$$

Equation (3.10) is satisfied if the tangential components of ψ are set to zero. As for the impermeable boundaries, this leads to a zero normal derivative for the normal component. The inlet boundary conditions for ψ may therefore be specified as

$$\psi_x = \psi_y = \frac{\partial \psi_z}{\partial z} = 0. \tag{3.11}$$

(c) *Outlet Boundary*

In determining the outlet boundary conditions, Eq. (3.4) is rewritten as

$$-\iint_{S_1} \mathbf{w}_0 \cdot d\mathbf{S}_1 = \iint_{S_2} (\nabla \times \boldsymbol{\psi} + \boldsymbol{w}_0) \cdot d\mathbf{S}_2 = Q, \tag{3.12}$$

where Q is the steady-state volumetric flow rate.

Noting that for a constant cross-sectioned duct,

$$-\iint_{S_1} \mathbf{w}_0 \cdot d\mathbf{S}_1 = \iint_{S_2} \mathbf{w}_0 \cdot d\mathbf{S}_2, \tag{3.13}$$

it follows that

$$\iint_{S_2} (\nabla \times \boldsymbol{\psi}) \cdot d\mathbf{S}_2 = 0. \tag{3.14}$$

To show that this condition is already satisfied by the prescribed solid boundary conditions, consider the exit plane as shown in Fig. 3.3 The edge values shown are those given by Eqs. (3.8) and (3.9). By Stokes' theorem, it is easily seen that

$$\iint_{S_2} (\nabla_\times \boldsymbol{\psi}) \cdot d\mathbf{S}_2 = \oint_{l_2} \boldsymbol{\psi} \cdot d\boldsymbol{l}_2 = 0. \tag{3.15}$$

This means that global continuity is satisfied irrespective of the interior values of ψ on the exit plane (assuming no discontinuities in ψ). On any boundary, however, ψ

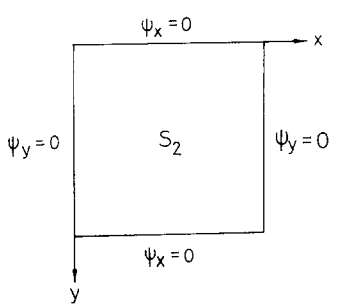

FIG. 3.3 The exit plane.

must be so derived that the velocity boundary conditions are satisfied. It is interesting to note that not all of the velocity components are required for such derivation. As demonstrated by Richardson and Cornish [14], two distinct sets of boundary conditions are possible depending on the choice of velocity components used. One, originally due to Hirasaki and Hellums [9], used only the normal velocity component, whereas the other, presented in [14], used only the tangential velocities at the boundaries. In a detailed investigation by Reizes *et al.* [15], it is pointed out that although neither set of formulations can guarantee no slip at the boundaries (due to numerical errors), the Hirasaki and Hellums approach at least enforces the prescribed normal velocity boundary conditions. Moreover, since the Richardson and Cornish formulation offers no such enforcement, the above workers encountered "leakage" through the boundaries whenever it was implemented in their enclosed convection models. With this in mind, the exit boundary conditions on ψ for the present model are developed by considering the axial velocity

$$w = \frac{\partial \psi_y}{\partial x} - \frac{\partial \psi_x}{\partial y} + w_0. \tag{3.16}$$

For the exit, fully developed conditions are assumed, so that

$$\frac{\partial w}{\partial z} = 0. \tag{3.17}$$

Differentiating Eq. (3.16) with respect to z and then substituting into Eq. (3.17) leads to

$$\frac{\partial^2 \psi_y}{\partial x \, \partial z} - \frac{\partial^2 \psi_x}{\partial y \, \partial z} = 0, \tag{3.18}$$

which is satisfied if on the exit plane

$$\frac{\partial \psi_x}{\partial z} = \frac{\partial \psi_y}{\partial z} = 0. \tag{3.19}$$

The final condition is then obtained from the solenoidal condition, so that

$$\frac{\partial \psi_z}{\partial z} = -\left(\frac{\partial \psi_x}{\partial x} + \frac{\partial \psi_y}{\partial y}\right). \tag{3.20}$$

Although the foregoing analysis is based on a duct of rectangular cross section, it may easily be extended to ducts of arbitrary but constant cross section. It should be noted that the boundary conditions for ψ on all except the exit plane have remained unchanged from those derived by Hirasaki and Hellums [9]; that is, zero normal derivatives and zero tangential components of ψ. For the exit plane, the relatively simple and readily implementable conditions Eq. (3.19) and Eq. (3.20) are applied.

Other Boundary Conditions

(a) *Velocity*

The velocity boundary conditions are straightforward and the usual assumptions of no-slip at the solid boundaries together with a uniform inlet profile are applied.

(b) *Vorticity*

Like the Vector Potential, the boundary conditions for vorticity have been a subject of much debate for some time. A multitude of formulations have been presented for two-dimensional studies, each claiming various advantages. (See Roache [10].) These include both first- and second-order schemes with some in terms of velocity and others related to the stream function and/or vorticity at interior mesh points. However, it is now generally accepted that the Woods formulation [16] is the most suitable for low to moderate Reynolds number flows in two dimensions. A similar approach is therefore adopted here, which leads to a second-order formulation of the boundary vorticities in terms of the Vector Potential. The final results differ from those derived earlier by Mallinson and de Vahl Davis [17] due to the improved treatment of the approximate $\psi - \zeta$ relationship near the boundaries.

Consider, for example, the boundary contained in the $x - z$ plane (Fig. 3.2). The Taylor series expansion of ψ_x at a mesh point adjacent to the boundary is given by

$$\psi_x(1) = \psi_x(0) + \Delta y \frac{\partial \psi_x}{\partial y}(0) + \frac{\Delta y^2}{2} \frac{\partial^2 \psi_x}{\partial y^2}(0) + \frac{\Delta y^3}{6} \frac{\partial^3 \psi_x}{\partial y^3}(0) + O(\Delta y^4), \tag{3.21}$$

where the indices 0 and 1 denote $y = 0$ and $y = \Delta y$, respectively.

The first term of the expansion is equal to zero since the tangential component of ψ vanishes on the impermeable boundary. The second term may readily be calculated numerically. But to avoid the necessity for a backward difference representation, it is noted that

$$w = \frac{\partial \psi_y}{\partial x} - \frac{\partial \psi_x}{\partial y} + w_0, \tag{3.22}$$

and since $w = 0$ on the boundary, the derivative in the second term may therefore be written as

$$\frac{\partial \psi_x}{\partial y}(0) = \frac{\partial \psi_y}{\partial x}(0) + w_0. \tag{3.23}$$

From Eq. (2.8) and Eq. (3.8), the second-order derivative in the third term may easily be identified as

$$\frac{\partial^2 \psi_x}{\partial y^2}(0) = -\zeta_x(0). \tag{3.24}$$

Finally, to obtain an expression for the fourth term, a linear distribution of vorticity over the first mesh interval is assumed, so that

$$\zeta_x = \zeta_x(0) + \frac{y}{\Delta y}\,[\zeta_x(1) - \zeta_x(0)]. \tag{3.25}$$

To approximate Eq. (2.8) over this interval, ζ_x is also written as

$$\begin{aligned}\zeta_x &= -\frac{\partial^2 \psi_x}{\partial y^2} + \frac{y}{\Delta y}\left[-\frac{\partial^2 \psi_x}{\partial x^2}(1) - \frac{\partial^2 \psi_x}{\partial z^2}(1)\right] \\ &= -\frac{\partial^2 \psi_x}{\partial y^2} + \frac{y}{\Delta y}\left[\zeta_x(1) + \frac{\partial^2 \psi_x}{\partial y^2}(1)\right].\end{aligned} \tag{3.26}$$

(This differs from the expression used in [17], where a less accurate representation $\zeta_x = -\partial^2 \psi_x / \partial y^2$ for $0 < y < \Delta y$ is assumed.)

Differentiating Eq. (3.26) with respect to y yields

$$\frac{\partial \zeta_x}{\partial y} = -\frac{\partial^3 \psi_x}{\partial y^3} + \frac{1}{\Delta y}\left[\zeta_x(1) + \frac{\partial^2 \psi_x}{\partial y^2}(1)\right]. \tag{3.27}$$

That is,

$$\frac{\partial^3 \psi_x}{\partial y^3} = -\frac{\partial \zeta_x}{\partial y} + \frac{1}{\Delta y}\left[\zeta_x(1) + \frac{\partial^2 \psi_x}{\partial y^2}(1)\right]. \tag{3.28}$$

From this, together with the assumption of linear variation of ζ over the first mesh interval, Eq. (3.25), it is seen that the third-order derivative in Eq. (3.21) may be written as

$$\frac{\partial^3 \psi_x}{\partial y^3}(0) = \frac{\zeta_x(0) - \zeta_x(1)}{\Delta y} + \frac{1}{\Delta y}\left[\zeta_x(1) + \frac{\partial^2 \psi_x}{\partial y^2}(1)\right]. \tag{3.29}$$

Substituting Eqs. (3.23), (3.24) and (3.29) into Eq. (3.21) leads to the relationship between the boundary vorticity and the Vector Potential, viz.,

$$\begin{aligned}\zeta_x(0) = &-\frac{3\psi_x(1)}{\Delta y^2} + \frac{3}{\Delta y}\left[\frac{\partial \psi_y}{\partial x}(0) + w_0\right] \\ &+ \frac{1}{2}\frac{\partial^2 \psi_x}{\partial y^2}(1) + O(\Delta y^2).\end{aligned} \tag{3.30}$$

For the z component of vorticity at this boundary, a similar technique is applied, resulting in

$$\zeta_z(0) = -\frac{3\psi_z(1)}{\partial y^2} + \frac{3}{\Delta y}\frac{\partial \psi_y}{\partial z}(0) + \frac{1}{2}\frac{\partial^2 \psi_z}{\partial y^2}(1) + O(\Delta y^2). \tag{3.31}$$

The third and final boundary vorticity may be deduced from the no-slip conditions and the definition of vorticity itself, Eq. (2.4), giving

$$\zeta_y(0) = 0. \tag{3.32}$$

Following the same approach, similar expressions may be found for the components of vorticity on the other boundaries.

Having established the necessary equations and boundary conditions the problem is now fully specified. All that remains is to implement an appropriate solution procedure in solving these equations.

4. Solution Procedure

All relevant equations (Eqs. (2.3), Eq. (2.8) and the corresponding boundary conditions) were transformed into their finite difference representations. The time derivatives appearing in the vorticity transport equations were replaced with forward differences whereas all spatial derivatives were represented by the second-order central difference approximations. The transient vorticity transport equations were conveniently solved using the Samarskii–Andreyev ADI scheme [18]. For the sake of accuracy, components of the Vector Potential were determined using the Discrete Fourier Analysis method [19], incorporating a Fast Fourier Transform algorithm.

In our test problems, a velocity field of $\mathbf{V} = w_0$ was specified as the initial conditions with all other fields set to zero. Where possible, however, the converged result for a Reynolds number of the same order of magnitude was used to initiate the solution process. The iterative cycle consists of the following:

(1) The three components of vorticity are obtained using Eq. (2.3).

(2) The x and y components of Vector Potential are determined from Eq. (2.8) with boundary conditions given by Eqs. (3.8), (3.9), (3.11) and (3.19).

(3) The z component of Vector Potential is then obtained using Eq. (2.8) with boundary conditions given by Eqs. (3.8), (3.9), (3.11) and (3.20).

(4) The components of velocity are then calculated using Eq. (3.1).

(5) New vorticity boundary conditions are obtained using Eqs. (3.30), (3.31) and (3.32).

(6) Test for convergence and, if necessary, return to (1). Since only the vorticity transport equations contain transient terms, the solution was considered converged when these terms diminish to some specified value, say, 10^{-5}.

5. Results and Discussion

The formulation proposed in this paper is applicable to incompressible flows in ducts with a arbitrary but constant cross section. Since abundant data are available for flows in square ducts, computations were carried out for such cases so that some meaningful evaluation of the method could be made. Results were obtained for a range of Reynolds numbers between 1 and 200. Typically, a mesh of $9 \times 9 \times 17$ was used for the lower Re(<100), while a $17 \times 17 \times 33$ grid was used for the higher Re cases. Due to geometric and dynamic symmetry, only one-quarter of the duct cross section was considered. The overall length of each duct was made sufficiently long so as to ensure, or at least approximate, fully developed conditions. To make efficient use of the computational nodes, the mesh transformation

$$Z = A \ln(B \cdot z + 1) \tag{5.1}$$

was applied to the axial coordinate in which

A and B are prescribed constants,

z is the actual coordinate in the axial direction, and

Z is the transformed coordinate.

Typically, the degree of transformation was chosen so that the first mesh interval in the z direction was approximately equal to mesh intervals in the x or y direction. Some numerical experiments have indicated that a transformed mesh of $17 \times 17 \times 33$ produces for all practical purposes identical results to those of a uniform grid of $17 \times 17 \times 65$. Such transformation represents a great saving in computational cost, which for reasons presented in Section 2 could not have been possible with the Hirasaki and Hellums formulation.

The centre line velocity gives some insight into the development of flow in the duct, and results for the various cases are presented in Fig. 5.1. The relatively slow development of a low Re flow is expected since mass and momentum are transferred

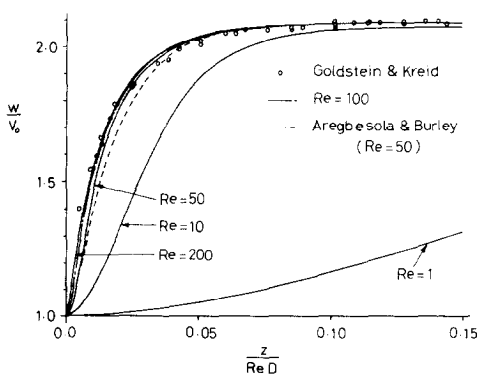

FIG. 5.1. Centre line velocity development.

principally by means of diffusion. When Re increases, the advection terms in the momentum equation take effect, until the flow becomes totally convective as $\mathrm{Re} \to \infty$. (Of course, turbulent conditions would prevent the occurrence of such a theoretical event.) What is unexpected, or at least not obvious, is how rapidly the flow development becomes characterised by the non-dimensional distance $z/(D\,\mathrm{Re})$, in which D is the hydraulic diameter. In Fig. 5.1, it is seen that, although there is substantial difference between the cases of $\mathrm{Re} = 10$ and 50, the results for $\mathrm{Re} = 100$ and 200 are virtually indistinguishable. From this, it is concluded that further increases in the Reynolds number would not cause any appreciable changes in the development characteristics. The excellent agreement between the current results for $\mathrm{Re} = 200$ and the experimental results of Goldstein and Kreid [20] as well as with other numerical solutions [21] serve to support such a conjecture.

Of the various duct flow models developed to date, most have employed the ideas of Patankar and Spalding [21], who assumed the flow to be parabolic. Although this assumption allows the use of a marching solution technique, it does limit the solution to high Reynolds numbers as well as restricting computations to cases where the axial velocity is everywhere positive. As a result, little information is available for flows at low Reynolds numbers. An extensive literature search yielded only the result of Aregbesola and Burley [13] for $\mathrm{Re} = 50$. This is shown as the broken line in Fig. 5.1. The discrepancies, particularly near the inlet region, are most probably attributed by the upwind differencing used by these authors. This technique, besides being unwarranted for such low Re, has the effect of artificially lowering the Reynolds number and hence may be the reason for their curve lying slightly below that of the present solution. Another factor which could have affected the accuracy of their solution is the use of a staggered grid system which necessitated averaging of advection terms in the vorticity transport equation. For example, the velocity in the term $u(\partial\zeta/\partial x)$ was calculated as the average of the velocities from eight neigbouring points. Such interpolation was not required in the present work since a single-coincident grid system was employed.

Velocity profiles are shown in Figs. 5.2 and 5.3 for two cases. As can be seen in the higher Re case, the agreement between the numerical results and the experimental

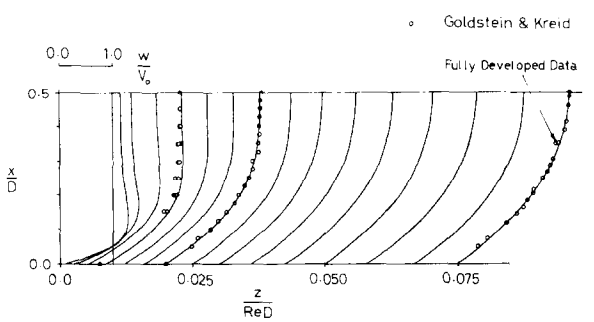

FIG. 5.2. Velocity profiles ($\mathrm{Re} = 100$).

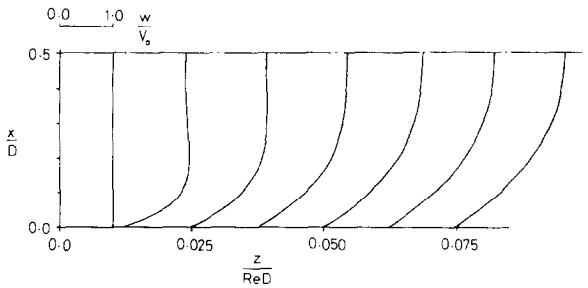

FIG. 5.3. Velocity profiles (Re = 10).

results [20] is excellent. An interesting feature of the computed profiles is the local maxima appearing near the walls which gradually approach the duct axis to form a single maximum. This phenomenon has been noted in many two-dimensional models. In particular, Friedman *et al.* [22] presented a detailed account on the possible causes of these "kinks." After some numerical experimentation with the inlet profiles, they concluded that the kinks are the results of the singularity imposed on the axial velocity at the leading edge. On the other hand, Abarbanel *et al.* [23] confirm the existence of these kinks as part of the analytical solution of the problem, and that they are not the results of numerical errors or the discontinuity of velocity at the inlet. Nguyen [24], by assuming the normal derivative of the entrance vorticity to be zero rather than setting the vorticity to zero in his parallel plate problem, was successful in removing the kinks, although this itself is no justification for using such unorthodox boundary conditions. Perhaps one sure way to resolve this mystery would be to carry out experiments which actually have inlet conditions as used in the numerical models.

In conclusion, a new formulation of the Vorticity–Vector Potential method for constant cross section duct flow problems is presented. Its capability in handling flows over a wide range of Re is demonstrated, and its potential in dealing with flow situations in which other models become inadequate is implied. For instance, it can handle low Reynolds number or recirculating flows for which the parabolic flow models are not applicable. It guarantees a zero divergence of velocity while the usual p, $\mathbf{V}$ method can at best approximate global continuity. Finally, it allows the efficient use of computational nodes while the commonly accepted Vector and Scalar Potential formulation requires a fine grid spacing at regions where little variation of velocity takes place.

REFERENCES

1. H. L. LANGHAAR, *Trans. ASME Ser. E J. Appl. Mech.* **9** (1942), A55.
2. L. S. HAN, *Trans. ASME Ser. E J. Appl. Mech.* **27** (1960), 403.
3. E. M. SPARROW, S. H. LIN, AND T. S. LUNDGREN, *Phys. Fluids* **7** (1964), 338.
4. G. A. CARLSON AND R. W. HORNBECK, *Trans. ASME Ser. E J. Appl. Mech.* **40** (1973), 25.

5. U. GHIA, K. N. GHIA, AND C. J. STUDERUS, *Comput. & Fluids* **5** (1977), 205.
6. G. DE VAHL DAVIS AND I. P. JONES, "Numerical Methods in Thermal Problems," Vol. II, p. 552, Pineridge Press, Swansea, United Kingdom, 1982.
7. K. AZIZ AND J. D. HELLUMS, *Phys. Fluids* **10** (1967), 314.
8. G. J. HIRASAKI AND J. D. HELLUMS, *Quart. Appl. Math.* **26** (1968), 331.
9. G. J. HIRASAKI AND J. D. HELLUMS, *Quart. Appl. Math.* **28** (1970), 293.
10. P. J. ROACHE, "Computational Fluid Dynamics," Hermosa Publishers, Albuquerque, N. Mex., 1972.
11. W. R. BRILEY, *J. Comput. Phys.* **14** (1974), 8.
12. S. DEL GIUDICE, M. STRADA, AND G. COMINI, *Numer. Heat Transfer.* **4** (1981), 215.
13. Y. A. S. AREGBESOLA AND D. M. BURLEY, *J. Comput. Phys.* **24** (1977), 398.
14. S. M. RICHARDSON AND A. R. H. CORNISH, *J. Fluid Mech.* **82** (1977), 309.
15. J. A. REIZES, E. LEONARDI, AND G. DE VAHL DAVIS, "Computational Techniques and Applications" (J. Noye and C. Fletcher, Eds.), p. 903, North-Holland Publ. Amsterdam, 1984.
16. L. C. WOODS, *Aero. Quart.* **5** (1954), 176.
17. G. D. MALLINSON AND G. DE VAHL DAVIS, *J. Comput. Phys.* **12** (1973), 435.
18. A. A. SAMARSKII AND V. B. ANDREYEV, *U.S.S.R. Computational Math. and Math. Phys.* **3** (1963), 1373.
19. R. C. LE BAIL, *J. Comput. Phys.* **9** (1972), 440.
20. R. J. GOLDSTEIN AND D. K. KREID, *Trans. ASME Ser. E, J. Appl. Mech.* **34** (1967), 813.
21. S. V. PATANKAR AND D. B. SPALDING, *Int. J. Heat Mass Transfer* **15** (1972), 1787.
22. M. FRIEDMAN, J. GILLIS, AND N. LIRON, *Appl. Sci. Res.* **19** (1968), 426.
23. S. ABARBANEL, S. BENNETT, A. BRANDT, AND J. GILLIS, *Trans. ASME J. Fluids Eng.* **92** (1970), 2.
24. T. V. NUGYEN, Ph.D. thesis, School of Mechanical and Industrial Engineering, University of New South Wales, Sydney, Australia, 1980.